Catal Lett (2008) 126:72–77
DOI 10.1007/s10562-008-9619-x

Selective N_2O Removal from the Process Gas of Nitric Acid Plants Over Ceramic $12CaO \cdot 7Al_2O_3$ Catalyst

Monika Ruszak · Marek Inger · Stefan Witkowski · Marcin Wilk · Andrzej Kotarba · Zbigniew Sojka

Received: 11 July 2008 / Accepted: 11 August 2008 / Published online: 9 September 2008

Abstract Catalytic high temperature decomposition (secondary abatement) of nitrous oxide over calcium aluminate $12CaO \cdot 7Al_2O_3$ (mayenite) was studied in the model laboratory tests (TPSR) and pilot units (steady-state) using the real feed. X-ray diffraction (XRD), scanning electron microscopy (SEM), N_2-sorption (BET), electron paramagnetic resonance (EPR) and Raman spectroscopies were used to characterize the synthesized material. The catalyst exhibited high efficiency and selectivity in N_2O removal, reaching practically 100% conversion at 1150 K without appreciable total losses of NO_x. Owing to its high thermal stability and resistivity to sintering and low cost of production raw materials, mayenite was found to be a promising catalyst for economically appealing secondary abatement of nitrous oxide in nitric acid plants.

Keywords Mayenite · N_2O decomposition · High temperature · Nitrous oxide · C12A7 · Pilot plant · Secondary abatement · Nitric acid · Process gas

1 Introduction

Nitric acid plants, where nitrous oxide is an undesired by-product are collectively the largest source of anthropogenic N_2O emissions (400 kt annually) in the chemical industry [1]. Mitigation of the nitrous oxide discharges, is thus becoming an urgent technological issue due to its contribution to greenhouse effect and stratospheric ozone destruction. The harmful effect of N_2O in the environment is reinforced by its long lifetime in the atmosphere of about 150 years and high global warming coefficient in comparison to other greenhouse gases such as CO_2 (310 times) or CH_4 (21 times). In this context, it is worth noting that abatement of nitrous oxide is simpler and less expensive than that of CO_2 and CH_4 [2].

In the nitric acid plant a typical process-gas composition is in the range: 95–97% of NO + NO_2, ca. 4% of N_2 and 1.5–2.5% of N_2O, and depends on the particular ammonia combustion conditions on Pt-Rh gauzes, catalyst composition and its age [1]. Once formed, nitrous oxide is not affected by the absorber and passes through the whole installation, contributing to the tail gas composition at the level of 300–3500 ppm [1].

There are basically two types of deN2O technologies available at the commercial scale: a non-catalytic (thermal decomposition in the enlarged reactor chamber) and a catalytic one (reduction and direct decomposition). Among the catalytic technologies the most interesting options are the high temperature (1073–1173 K) abatement from the process-gas, and the low temperature (473–573 K) elimination of N_2O from the tail gas [1].

The high temperature process-gas solution is one of the most cost-effective and easy in the application from the technological point of view. The catalyst can be placed simply just after the Pt—Rh gauze in the existing burner, without making any noticeable modifications in the installation. Primary requirements for a suitable catalyst are high activity and selectivity in N_2O decomposition (conversion >90% with simultaneous passivity towards

The work was presented during the conference Catalysis for Society, Krakow, May 11–15, 2008.

M. Ruszak · S. Witkowski (✉) · A. Kotarba · Z. Sojka
Faculty of Chemistry, Jagiellonian University, ul. Ingardena 3, 30-060 Krakow, Poland
e-mail: witkowss@chemia.uj.edu.pl

M. Inger · M. Wilk
Instytut Nawozow Sztucznych, al. 1000-lecia Panstwa Polskiego 13A, 24-110 Pulawy, Poland

NO) and durability in reaction conditions, where sintering plays an important role. Although several systems exhibit sufficient activity, only few materials can survive severe process conditions. Volatilization, corrosion and solid state reactions between the active phase and support are among the principal reasons leading to progressive catalyst deterioration. The most important catalytic systems reported in the literature include supported oxides (CuO/Al_2O_3 [3] and Co_2AlO_4/CeO_2 [4]), perovskite ($La_{0.8}Ce_{0.2}CoO_3$ [5]) and hexaaluminate $ABAl_{11}O_{19}$ (A = La, Ba, B = Mn, Fe, Ni) [6]. However, in contrast to extensive research dealing with the tail gas deN_2O, little work has been performed on the process-gas option. In the present study we explored the possibility of using mayenite as a robust ceramic catalyst for the high temperature N_2O decomposition.

Mayenite, often labeled as C12A7, is a nanoporous calcium aluminate ($12CaO \cdot 7Al_2O_3$) with extra-framework oxygen anions. This refractory ceramic material can be prepared by calcination of stoichiometric mixtures of calcia and alumina at temperatures around 1600 K [7]. The framework of mayenite is composed of densely packed, interconnected cages (Fig. 1), similar to those found in zeolites, but with the positive electric charge (equivalent to +1/3e per each cage). The cages are occupied by various extraframework anions satisfying the overall electroneutrality condition. Due to the space confinement, the guest species are limited to mono or diatomics such as O^{2-}, O^-, O_2^-, O_2^{2-}, OH^- [8].

The ability of storing large amount of oxygen in the bulk is the unique property of mayenite [9]. The most promising for catalysis is the fact that the encaged oxygen species can migrate between the surface and the bulk. They can be thus gradually released at elevated temperatures (in oxygen lean conditions) or stored (in oxygen reach conditions), and possibly take part in catalytic reactions in an atypical fashion. Therefore, the reported catalytic properties of mayenite have often been associated with its strong oxidation ability, presumably involving the clathrated oxygen, in the number of processes such as partial oxidation of methane to syngas [10], soot combustion [11], or pyrolysis of methylcyclohexane [12].

The low surface area of mayenite produced by ceramic method is usually one of the important constraints, restraining its wide use for typical catalytic purposes. However, it can be a clear advantage for high temperature applications in selective removal of N_2O from the process gas in nitric acid plants provided that the catalyst exhibits sufficient activity to assure the desired complete conversion.

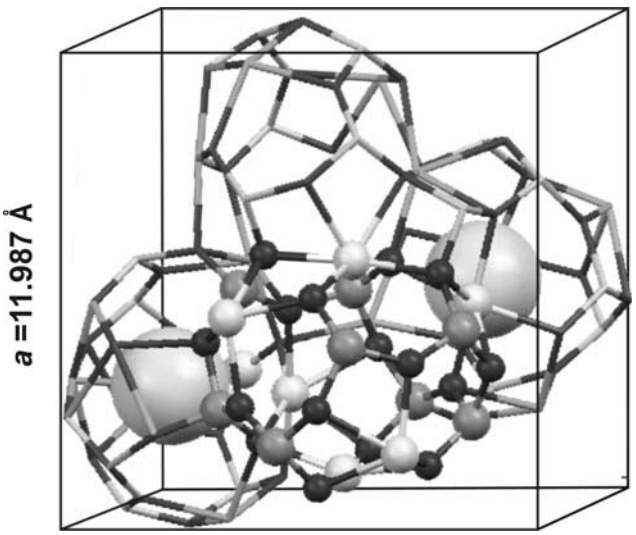

Fig. 1 Unit cell of mayenite structure, showing the interconnected nanocages. The large grey spheres indicate the extra-framework ionic positions, calcium ions are labeled white, aluminum are grey and oxygens are black

2 Experimental

2.1 Materials

Polycrystalline samples of mayenite were prepared according to conventional ceramic procedure from analytical grade $CaCO_3$ (Aldrich) and γ-Al_2O_3 (Aldrich). Both reactants were mixed in the stoichiometric ratio (12:7) and milled in an electromechanical agate mortar for about 6 h. Homogenized samples were annealed at 1620 K in a tubular furnace for 6 h in air [13].

2.2 Techniques

The phase composition of the mayenite samples was examined by X-ray diffraction, using CuKα radiation ($\lambda_{\alpha 1} = 1.5406$ Å, $\lambda_{\alpha 2} = 1.5444$ Å) by means of a Philips XPERT PRO PW1710 diffractometer. Data were recorded in the 2θ range of 10–80° with the resolution of 0.02°. The sample morphology was investigated by a Hitachi S-4700 microscope, equipped with a Noran Vantage microanalysis system. Prior to the experiments the samples were carbon coated.

BET surface area of mayenite samples was measured by N_2 adsorption, using Quantasorb Jr. system (Ankersmit). The samples were dried at 520 K under flow of N_2 before the measurements.

Evolution of the paramagnetic extraframework anions in the temperature range 293–1173 K, was studied by EPR method. The spectra were recorded at liquid nitrogen temperature on a Bruker ELEXYS 500 X-band spectrometer with 100 kHz modulation. The EPRsim32 program was used for computer simulation of the experimental spectra [14].

Diamagnetic O_2^{2-} and OH^- species were identified with Raman spectroscopy using Jobin Yvon T64000 instrument, equipped with a CCD3000 detector and an Ar laser (2025 Spectra Physics) operating at the wavelength of 514.5 nm with the resolution of 4 cm^{-1}.

The temperature programmed surface reactions of N_2O and NO decompositions were performed in a fixed-bed flow reactor, equipped with QMS detector (SRS RGA200, Stanford Research System). The QMS signals for m/z of 44, 30, 28, 32 and 18 corresponding to N_2O, NO, N_2, O_2 and H_2O, respectively, were monitored. Individual runs were carried out in the temperature range of 300–1200 K, either in the flow of 5% N_2O/He or in 1% NO/He both with GHSV of 7000 h^{-1} and the temperature rate of 10 K/min. The mass of mayenite samples was 150 mg and the catalyst was prepared as a sieve fraction of 0.2/0.3 mm.

Catalytic tests of N_2O decomposition using a real feed (850 ppm N_2O, 8.15% vol. NO, 2.5% vol. NO_2, 15–20% vol. H_2O, 4.5–4.8% vol. O_2 and N_2 as a balance) were performed in a by-pass reactor connected to the pilot plant. Approximately 2 g of the mayenite sample (sieve fraction 0.5/0.6 mm) was placed in the reactor (id. 10 mm). The inlet stream of the process gases was taken directly from the pilot plant. In order to prevent condensation of water in the feed the entire transfer line was heated. Isothermal steady state catalytic tests were carried out at 1070 and 1150 K. Gas composition (at the inlet and outlet of the reactor) was analyzed with an infrared detector (GAS-MET). During the experiments the GHSV value of the feed was kept at 100,000 h^{-1}, which is in the range of the values actually used in industry.

3 Results and Discussion

3.1 Catalyst Characterization

Typical X-ray diffraction pattern of the synthesized samples is shown in Fig. 2a. The principal lines of the mayenite phase were indexed within the $I\bar{4}3d$ space group (PDF WIN 62040-ICSD). Apart from the major mayenite phase, two spurious minor phases ($Ca_3Al_2O_6$ and $CaAl_2O_4$) can also be recognized in the XRD pattern. They are the usual impurities formed during the synthesis of mayenite, as can be inferred from the corresponding phase diagram of the CaO–Al_2O_3 binary system [15].

A representative SEM image of the investigated samples is shown in Fig. 2b. The observed sub-micron crystals ($\sim$0.08 μm) are sintered into larger aggregates of 2–10 μm in size. Blunt shaped edges indicate that partial surface melting at the synthesis temperature took place. The specific BET surface area of the resultant ceramic catalyst is quite low (around 1 m^2/g), which should be beneficial for a durable catalyst supposed to work at high temperatures.

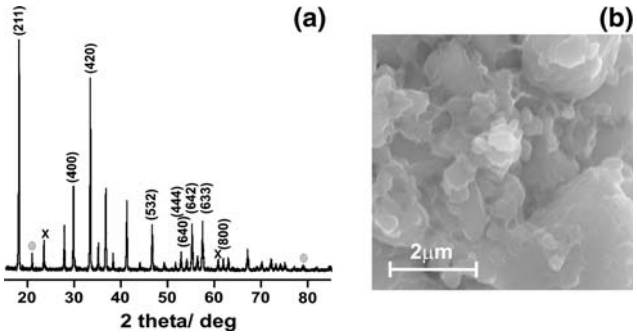

Fig. 2 Characterization of the synthesized mayenite catalyst: (**a**) X-ray diffraction pattern of the mayenite phase with Miller indices (hkl) indicated for selected peaks. The residual phases $Ca_3Al_2O_6$ and $CaAl_2O_4$ are marked with a grey circle and cross, respectively. (**b**) 20 keV SEM image obtained with secondary electrons

The encaged counter-ions were identified by EPR and Raman spectroscopies. In Fig. 3a (solid line) the EPR spectrum of the paramagnetic O_x^- ($x = 1$, 2) species is shown. Computer simulation allowed for decomposition of this spectrum into two components signals due to O^- ($g_{xx} = 2.054$, $g_{yy} = 2.025$, $g_{zz} = 2.014$) and O_2^- ($g_{xx} = 2.005$, $g_{yy} = 2.012$, $g_{zz} = 2.078$) radicals (doted lines) [13]. The OH^- anions were identified based on Raman spectroscopic fingerprints of 3621 and 3675 cm^{-1} (Fig. 3b). In the case of diamagnetic O_2^{2-} anions the situation is more subtle since the Raman characteristic peak at 771 cm^{-1} is superimposed on 773 cm^{-1} band associated with AlO_4 tetrahedrons [16, 17] (Fig. 3c). Nonetheless, the intensity of this compound maximum substantially changes upon treatment in oxygen lean and oxygen reach

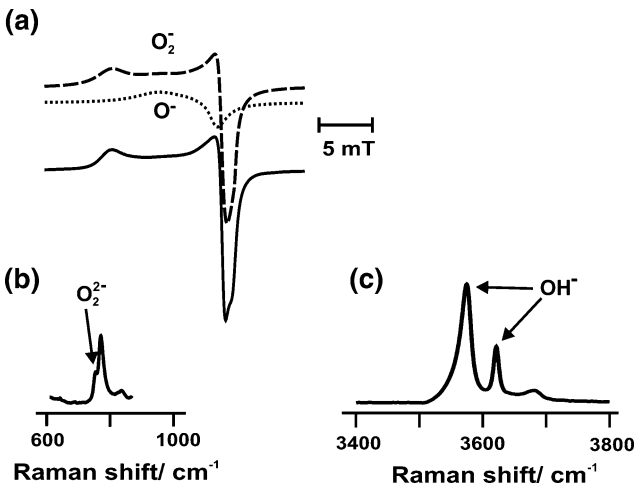

Fig. 3 Spectroscopic characterization of extra-framework anions present in mayenite. (**a**) EPR spectrum of O_x^- species (solid line) and the simulated components signals of O^- and O_2^- radicals (dashed lines). Raman spectra of (**b**) O_2^{2-} and (**c**) OH^- cage species

conditions, indicating that the component associated with the O_2^{2-} cage species has a sizable contribution to this peak.

3.2 Catalytic Tests

Preliminary catalytic tests of N_2O and NO decomposition were performed in the laboratory scale in the TPSR regime using 5% N_2O/He and 1% NO/He reaction gas mixtures, respectively. The results of both tests are shown together in Fig. 4 for compactness, along with the corresponding temperature profile. Appreciable conversion of N_2O was observed above 850 K and upon reaching the process temperature (1150 K) the decomposition of nitrous oxide achieved ca. 90% (Fig. 4a). The reactivity of the empty reactor was checked in a blank experiment and revealed that the onset of the N_2O decomposition (1050 K) is shifted by 300 K towards higher temperatures (Fig. 4b), in accordance with previously reported data [6]. In a parallel experiment the concentration of NO during the whole temperature range remains essentially constant within the experimental error. The TPSR data, expressed as N_2O conversion (X_{N_2O}) versus temperature (T) were fitted with the kinetic model described elsewhere [18]:

$$X_{N_2O} = 1 - \exp(-k/\mathrm{GHSV}) \quad (1)$$

with the rate constant given by the Arrhenius formula $k = Ae^{-(E_a/RT)}$, where E_a is the activation energy. The fit to the experimental curve is shown in the insert in Fig. 4a. The applied model reproduced the experiment quite well, indicating that the kinetic relaxation of the catalytic system is sufficiently fast in comparison to the rate of the temperature increase, so the presumed quasi steady-state is likely to be approached. The value of the apparent activation energy was found to be 120 ± 5 kJ/mol, whereas for the thermal decomposition is about 250 kJ/mol [19]. The observed activation energy is close to that found for the barium and iron modified aluminate catalyst (100 kJ/mol) for high temperature deN_2O [6].

Physical characteristics and promising laboratory scale results with pure gases suggested that mayenite should be a good candidate as a robust catalyst for the industrial process-gas option. In order to evaluate its potential capacity the high temperature tests on real feed were carried out in a specially design by-pass reactor of the pilot plant of the nitric acid production (Pulawy). Such set-up allowed for unique opportunity to test the catalyst performance with a genuine industrial process gas composition and space velocity. The results of isothermal steady state screening performed at 1070 and 1150 K are shown in Fig. 5. In the case of N_2O decomposition the conversion of 60% at 1070 K was observed, whereas at 1150 K it reached 99.7%. Partial transformation of NO_2 into NO that took

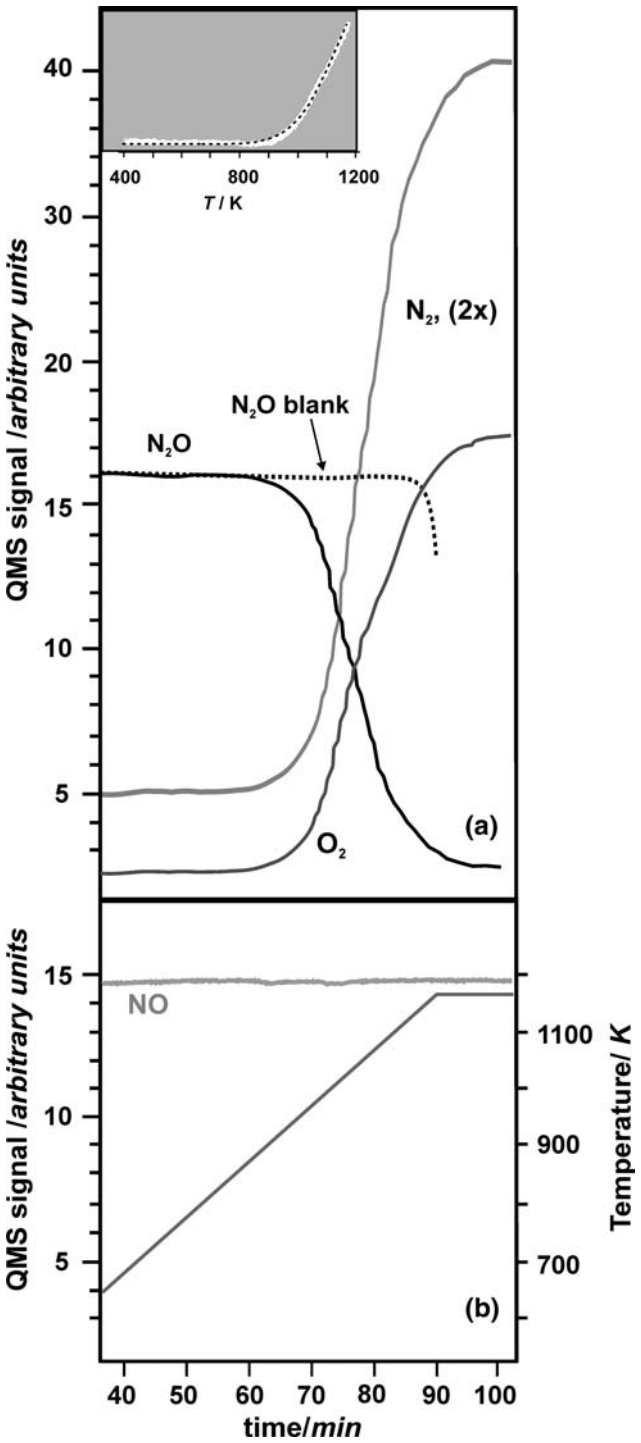

Fig. 4 (**a**) TPSR profiles for N_2O decomposition tests performed in laboratory scale over mayenite along with the associated N_2 and O_2 lines. The doted line represents the blank experiment, whereas in the insert the kinetic fit (black dotted line) to the experimental data (white dotes) is shown. (**b**) The NO line with the temperature profile used in all the TPSR experiments

place, upon passing to higher temperature, was mainly due to the shift of the thermodynamic equilibrium. However, the NO_x balance was nicely preserved (slightly negative at

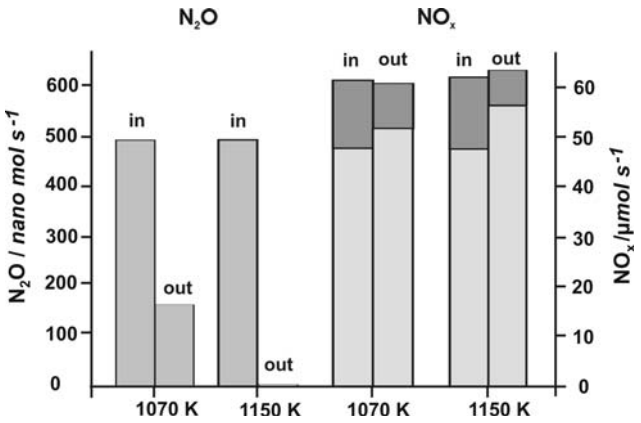

Fig. 5 Catalytic screening of N_2O decomposition performed in a pilot plant at 1070 and 1150 K using real process gas feed. The bars represent the N_2O and NO (light grey) and NO_2 (dark grey) compositions in the inlet and outlet of the reactor

lower and positive at higher test temperature) within the experimental error. These results indicate that at the process condition temperature (1150 K) nitrous oxide is completely and selectively decomposed over ceramic mayenite catalyst, whereas the total content of the target NO_x gases was retained. The test revealed that the catalyst activity was sustained at 1050 K for at least 10 h.

3.3 Mechanistic Considerations

For the N_2O decomposition over oxide catalysts not containing transition metal ions the anionic redox mechanism initiated by the oxygen atom transfer was proposed [20]. It consists of two principal reaction steps: N–O bond breaking via oxygen atom transfer to the surface with formation of the peroxy intermediate ($N_2O + {O^{2-}}_{surf} \rightarrow {O_2^{2-}}_{surf} + N_2$) and O–O bond formation by recombination of oxygen atoms into dioxygen via surface diffusion of peroxy species (${O_2^{2-}}_{surf} + {O_2^{2-}}_{surf} \rightarrow 2{O^{2-}}_{surf} + O_2$). The catalyst reactivity is thus related to the ability of surface oxygen anions to efficiently abstract the oxygen atom from N_2O molecule and to foster diffusive recombination of the ad-oxygen intermediates. In this context the peculiar feature of mayenite, with its large capacity for storage of the sub-surface oxygen species, opens two interesting mechanistic pathways. They consist in suprafacial recombination of surface peroxy ions (as shown above) and intrafacial recombination of surface peroxy with cage and surface oxygen species (${O_2^{2-}}_{surf} + {O_2^{x-}}_{cage} \rightarrow O_2 + {O^{2-}}_{surf} + {O^{x-}}_{cage}$). Both routs are depicted at the atomic scale in the structural context of mayenite in Fig. 6a and b, respectively. The necessary condition for the intrafacial mechanism to be actually triggered is an efficient oxygen transport between the surface and the cage sites at the high temperature deN_2O reaction. This issue was addressed by

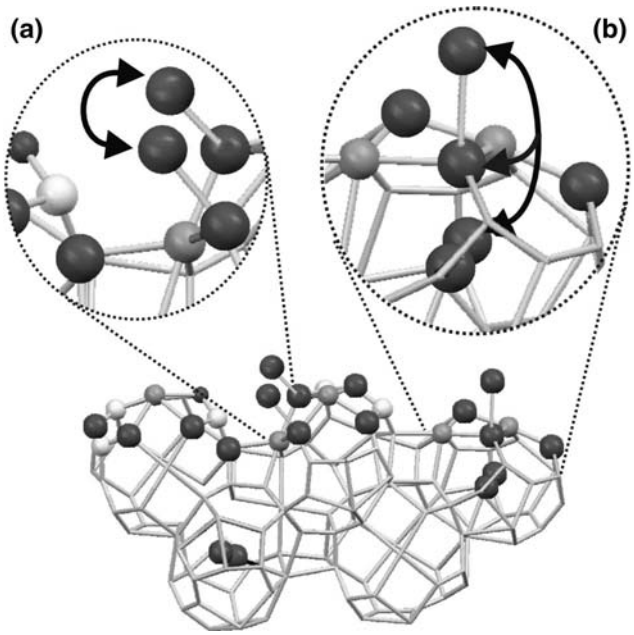

Fig. 6 Schematic view of the postulated (**a**) suprafacial and (**b**) intrafacial recombination of oxygen atoms produced upon dissociation of N_2O over the mayenite catalyst. The arrows indicate the oxygen atoms involved in the recombination process

complementary EPR and oxygen storage and release evaluation experiments. A sample of mayenite was depleted of cage dioxygen species in a soot combustion experiment under the flow of He. The gas phase composition monitored by QMS showed that the maximum CO_2 profile appears around 1100 K (Fig. 7a), indicating that indeed at the deN_2O process conditions the stored oxygen can be effectively supplied to the surface of the mayenite catalyst. The reverse process of oxygen storage in the mayenite cages was investigated in an EPR experiment, where the depleted sample was heated up to 1170 K in the presence of N_2O. Whereas for the oxygen lean catalyst no EPR signal due to encaged oxygen radicals was detected (Fig. 7b), in the case of mayenite after the treatment in N_2O at the process temperature a strong signal of O_x^- radicals appeared (Fig. 7c). These results show clearly that the oxygen species located in the near-to-surface region can be easily stored and released above 1000 K. The clathrated oxygen can thus shuttle between the surface and cage sites of the mayenite and participate effectively in the catalytic processes. Taking into account that the activation energy determined for oxygen diffusion in mayenite (67.5 kJ/mol [21]) is much lower than the activation energy of N_2O decomposition, such mechanism seems to be quite plausible. It could compensate the low surface area of the ceramic catalyst enhancing its activity. More detailed isotopic experiments are planed to definitely resolve the actual involvement of both recombination pathways in the real deN_2O reaction conditions.

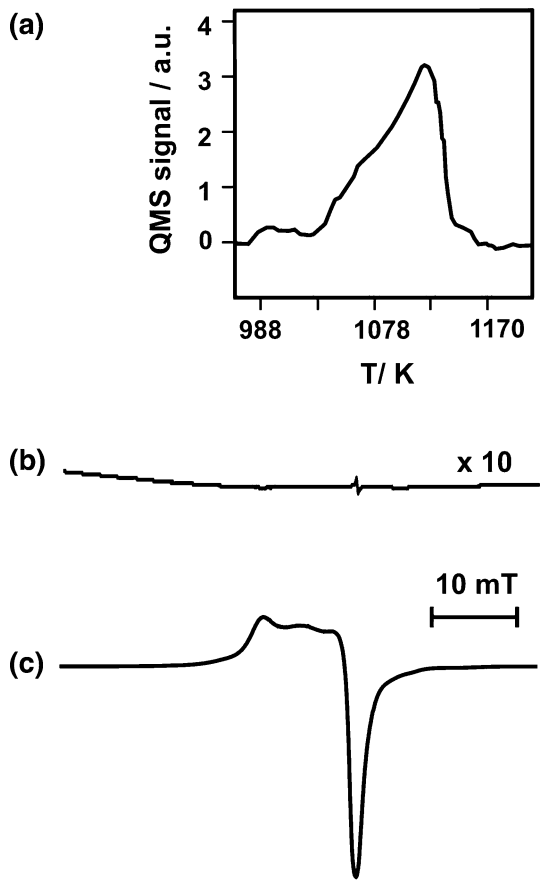

Fig. 7 (**a**) The QMS-CO_2 profile of TPRS studies of oxygen storage using soot as a test material. (**b**) EPR spectra of oxygen lean and (**c**) oxygen reach mayenite

4 Conclusions

The new mayenite ceramic catalyst for high temperature decomposition of nitrous oxide in process gases shows excellent performance and fulfills the activity and selectivity requirements for industrial applications in nitric acid plant secondary abatement. At averaged temperature of the ammonia burner (1150 K) practically 100% conversion of N_2O was achieved, with the total NO_x yield being well preserved. The low surface area (1 m^2/g) and refractory character of mayenite augur well for its future successful application as a promising alternative to the patented catalysts, such as ceria supported Co_2AlO_4 spinel or ceria promoted cobalt lanthanum perovskite.

References

1. Pérez-Ramírez J, Kapteijn F, Schöffel K, Moulijn JA (2003) Appl Catal B Environ 44:117
2. Centi G, Perathoner S, Vazzana F (1999) Chemtech 29:48
3. Schumacher V, Buerger G, Fetzer T, Baier M, Hesse M (1999) (BASF) Patent WO9955621
4. Nirisen O, Schoffel K, Weller D, Ovrebo D (2002) (Yara International) Patent WO0202230
5. Axon SA, Coupland DR, Horner BT, Ridland J, Wishart IC (2004) (Johnson Mattey) Patent WO04096702A2
6. Santiago M, Pérez-Ramírez J (2007) Environ Sci Technol 41:1704
7. Yang S, Kondo JN, Hayashi K, Hirano M, Domen K, Hosono H (2004) Chem Mater 16:104
8. Trofymluk O, Toda Y, Hosono H, Navrotsky A (2005) Chem Mater 17:5574
9. Hayashi K, Hirano M, Matsuishi S, Hosono H (2002) J Am Chem Soc 124(5):738
10. Yang S, Kondo JN, Hayashi K, Hirano M, Domen K, Hosono H (2004) Appl Catal A Gen 277:239
11. Sato K, Yamaguchi M, Fujita S, Suzuki K, Mori T (2006) Catal Commun 7:132
12. Pant K, Kunzru D (1998) Chem Eng J 70:47
13. Ruszak M, Witkowski S, Sojka Z (2007) Res Chem Intermed 33:689
14. Spałek T, Pietrzyk P, Sojka Z (2005) J Chem Inf Model 45:18
15. Zawrah MF, Khalil NM (2006) Ceram Int 33(8):1419
16. Che M, Tench AJ (1983) Adv Catal 32:1
17. Kajihara K, Matsuishi S, Hayashi K, Hirano M, Hosono H (2007) J Phys Chem C 11:14855
18. Chang KS, Song H, Park Y-S, Woo J-W (2004) Appl Catal A Gen 273:223
19. Bamford CH, Tipper CFH (1972) Reaction of non-metallic inorganic compounds, vol 6. Elsevier, Amsterdam, p 65
20. Pietrzyk P, Zasada F, Piskorz W, Kotarba A, Sojka Z (2007) Catal Today 119:219
21. Li Q, Hosono H, Hirano M, Hayashi K, Nishioka M, Kashiwagi H, Torimoto Y, Sadakata M (2003) Surf Sci 527:100